1_C37

Numerical analysis of airflow dynamics generated by human coughing based on PIV experimental results

Wonseok Oh, PhD

Ryozo Ooka, PhD
Member ASHRAE

Hideki Kikumoto, PhD
Member ASHRAE

Mengtao Han, PhD

ABSTRACT

Respiratory infections are transmitted by droplets and droplet nuclei generated by human coughing, sneezing, and talking. Droplets and droplet nuclei come out of the mouth simultaneously with airflow, and their dispersion characteristics are important to understand the transmission route of infection. It is crucial to understand the dispersion characteristics of droplets and droplet nuclei dispersion and infection routes through numerical analysis. The present study aims to provide boundary conditions of the computational fluid dynamics (CFD) model to confirm the prediction accuracy of CFD analysis of human coughing based on the experimental results of particle image velocimetry (PIV). The projection area of the mouth, which is the boundary condition of airflow generated by human coughing, was assumed as an ellipse shape, major axis length was 43.2 mm (1.7 in), and the ratio of the major and minor axis was 4. Because the air velocity corresponding to the boundary condition of the mouth in the CFD model cannot be derived directly from the PIV results, the time-series airflow distribution was analyzed by introducing a correction factor, and the boundary condition with the smallest error with the experimental result was inversely derived. As a result, the airflow generated by coughing with CFD analysis could be reproduced with an RMSE of 0.38–0.42 m/s (1.25–1.38 ft/s) compared to the ensemble average obtained in the experiment. This study provides detailed modeling techniques and boundary conditions of numerical simulation for analyzing the airflow characteristics generated by human coughing. In addition, it is expected that the risk and route of infection caused by human coughing can be predicted through CFD analysis by additionally measuring the size distribution of droplets and droplet nuclei and introducing Lagrangian analysis.

INTRODUCTION

Investigating the dynamic characteristics of droplets and droplet nuclei generated by respiratory activities, which are viral infectious particles, is very important in understanding a transmission route and establishing infection prevention and control measures. Droplet sizes have been reported to be 0.1–500 μm for coughing, 0.1–125 μm for talking, and 1.0–125 μm for sneezing (Gralton et al. 2011). Likewise, because the size of the particles ejected from the respiratory activity is very small and the evaporation phenomenon occurs on the particle surface, it is difficult to continuously track them. The computational fluid

Wonseok Oh is a research fellow in the Institute of Industrial Science, the University of Tokyo, Japan. **Ryozo Ooka** is a professor in the Institute of Industrial Science, the University of Tokyo, Japan. **Hideki Kikumoto** is an associate professor in the Institute of Industrial Science, the University of Tokyo, Japan. **Mengtao Han** is an associate professor in Huazhong University of Science and Technology, China

dynamics (CFD) method could be an effective manner to analyze the movement of particles and investigate the infection risk caused by dispersed infectious particles. Additionally, many studies already utilized the CFD method to investigate the infection risk (He et al. 2011; Richmond-Bryant 2009; Qian and Li 2010) and to confirm the possibility of airborne infections as indirect evidence (Yu et al. 2004).

When simulating respiratory activity using CFD, not only the droplets, which are infectious particles, but also the characteristics of the exhaled airflow that affect the kinetic properties of the droplets and droplet nuclei should be taken into account. Airflow characteristics of coughing and sneezing are difficult to measure because they form over a very short period, approximately 0.3–0.8 seconds (Gupta, Lin, and Chen 2009; Scharfman et al. 2016). As a suitable method for detecting such a very rapid airflow change, three techniques are largely used: Schlieren imaging technique (Xu et al. 2017), spirometer (Gupta, Lin, and Chen 2009), and particle image velocimetry (PIV). The Schlieren imaging technique is good to understand the overall flow pattern but obtained air velocity may smaller than the actual air velocity. Meanwhile, Gupta et al. used a spirometer to measure the airflow rate caused by coughing and proposed a coughing model using a gamma probability distribution. In addition, this cough model has been the most widely used as a CFD boundary condition. However, the measurement of the airflow rate using a spirometer has a disadvantage in that a pressure loss occurs due to the connection pipe between mask and spirometer. Moreover, it is different from the airflow that forms naturally by coughing, and airflow distribution patterns cannot be identified. The PIV technique has the advantage of not only obtain air speed results that can be directly used for the boundary conditions in CFD simulation but also confirm the naturally diffused airflow patterns in the space.

Therefore, the objectives of the present research are to investigate the airflow results obtained from the PIV experiment and grasp the boundary condition of CFD simulation that can reproduce the human coughing. The results of this study are expected to be used as a basic method to evaluate the infection risk through the application of droplets and droplet nuclei dispersion analysis by reproducing the airflow caused by coughing close to the actual phenomenon.

METHODOLOGY

Air speed characteristics generated by human coughing

In order to adopt the air speed results obtained from the PIV experiment to boundary conditions in CFD simulation, the time-series air speed characteristics generated from coughing were redefined as shown in Figure 1. PVT, PV, and CDT represent peak velocity time of coughing, peak velocity, and coughing duration time, respectively.

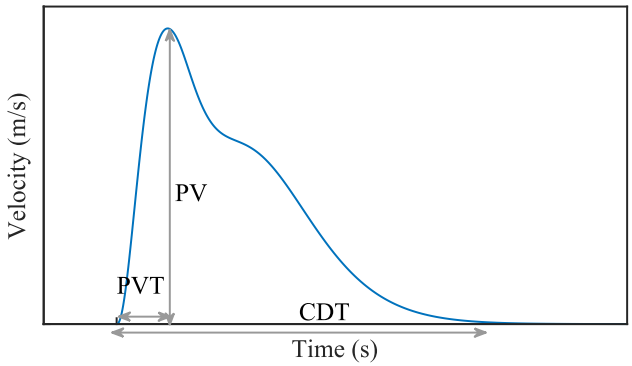

Figure 1 Time-series air velocity characteristics generated from coughing. PVT: peak velocity time, PV: peak velocity, CDT: coughing duration time

Analysis of experimental results

Our previous experiment results were analyzed to establish boundary conditions for the reproduction of airflow generated by coughing (Han et al. 2021). The left side Figure 2 shows a schematic diagram Pof the PIV experiment. The 15 sets of time-

series airflow distribution in horizontal and vertical planes were obtained, respectively. The center of the mouth, where airflow was ejected by coughing, was set as the origin (0,0,0) of the coordinates. Airflow characteristics caused by coughing were formed very differently for everyone. Therefore, the velocity magnitude v_i, space (x, y, z), and time t were normalized by PV, mouth width of each individual b_i, and PVT_i , respectively as shown in Equations (1) and (2). The mean and deviation of the mouth width of participants were 43.2 ± 5 mm (1.7 ± 0.2 in). The ensemble average was calculated using the normalized V_i^{vertical} and $V_i^{\mathrm{horizontal}}$ by Equation (3).

$$V_i^{\mathrm{vertical}} = \left\{\frac{v_i}{\mathrm{PV}_i}, \left(\frac{x}{b_i}, \frac{z}{b_i}\right), \frac{t}{\mathrm{PVT}_i}\right\} \quad (1)$$

$$V_i^{\mathrm{horizontal}} = \left\{\frac{v_i}{\mathrm{PV}_i}, \left(\frac{x}{b_i}, \frac{y}{b_i}\right), \frac{t}{\mathrm{PVT}_i}\right\} \quad (2)$$

$$\langle V \rangle = \frac{1}{N}\sum_{i=1}^{N} V_i \quad (3)$$

Table 1 shows the characteristics summary of airflow. The position at x/b = 2.5 was set as a reference because the airflow velocity was most clearly visible. There was no significant difference between the vertical and horizontal planes, and the maximum wind speed was around 10.8–11.4 m/s (35.5–37.2 ft/s).

Table 1. Average airflow characteristics generated from coughing (x/b = 2.5)

	Vertical	Horizontal	Overall
Number of data	30	30	60
PV [m/s (ft/s)]	10.81 (35.47)	11.35 (37.24)	11.08 (36.35)
PVT (s)	0.019	0.018	0.019
CET (s)	0.605	0.485	0.545

The right side of Figure 2 shows the normalized ensemble average results at x/b = 2.5 position in the vertical and horizontal planes. The root-mean-square error (RMSE) between results of vertical and horizontal was 0.031. The normalized ensemble velocity can be converted to an actual scale using the mean PV and PVT to obtain the time-series velocity data generated by coughing. The normalized space x/b = 2.5 represents the 108 mm which is far from the mouth and can not be used directly as a boundary condition in CFD. Therefore, in order to reproduce the airflow caused by coughing using the CFD method, the time-series velocity obtained at x/b = 2.5 should be adjusted and used as a boundary condition and used for verification.

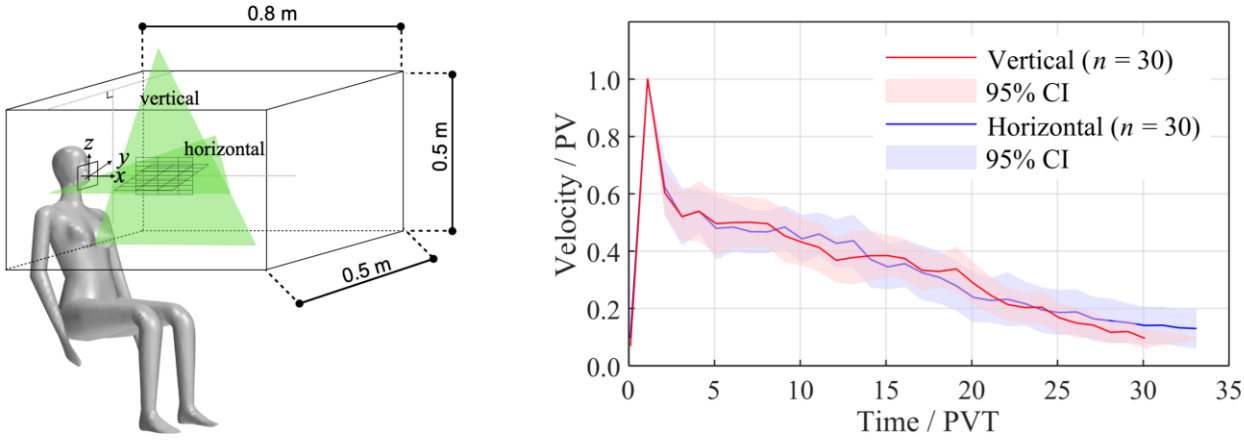

Figure 2 Schemati diagram of PIV experiment and result of air velocity at $x/b = 2.5$.

Ensemble avreage of coughing airflow distributions

In the experiment, the mouth location of subject for coughing was fixed, and the subjects tried to form an airflow straight forward as possible as they can, but the direction of the airflow was formed differently by the position and lip shape of subjects. Therefore, it is not appropriate to average the airflow distribution without any processing, and the airflow velocity distribution in the space obtained from the image was averaged by aligning the airflow direction with coordinate axes rotation and translation as shown in Figure 3. In the time-series ensemble average result, the values at Points 1–4, which are the position of x/b = 2.5, are used to verify the CFD calculation result.

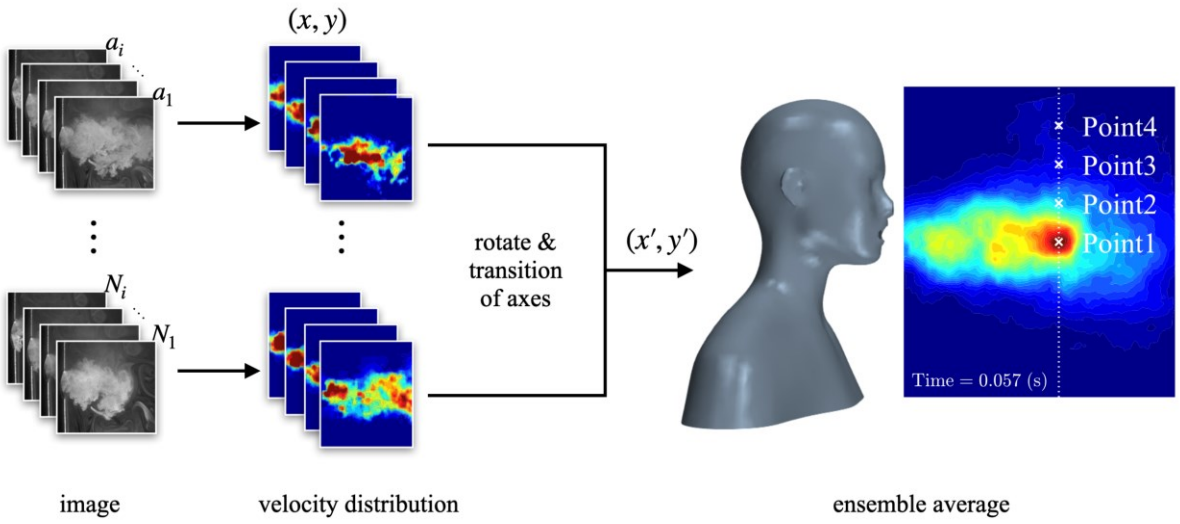

Figure 3 Schematic diagram of emsemble average of coughing airflow distribution measured by PIV.

Numerical simulation design

In CFD analysis, a room with a size of 3.0 × 2.0 × 2.4 m^3 (9.8 × 6.6 × 7.9 ft^3) was considered, and a human model and the same acrylic chamber (0.8 × 0.5 × 0.5 m^3 (2.6 × 1.6 × 1.6 ft^3)) were placed in the center of the room as same as the experiment as shown in Figure 4. The shape of the mouth of the human model was assumed to be an ellipse with an aspect ratio of 4. The average mouth width obtained by the experiment was 43.2 mm (1.7 in) and the mouth area was set as 363.9 mm^2 (0.56 in^2) in the human model. In previous studies, the area of mouth during coughing was reported 337–400 mm^2 (0.52–0.62 in^2) (Zhu, Kato, and Yang 2006; Gupta, Lin, and Chen 2009).

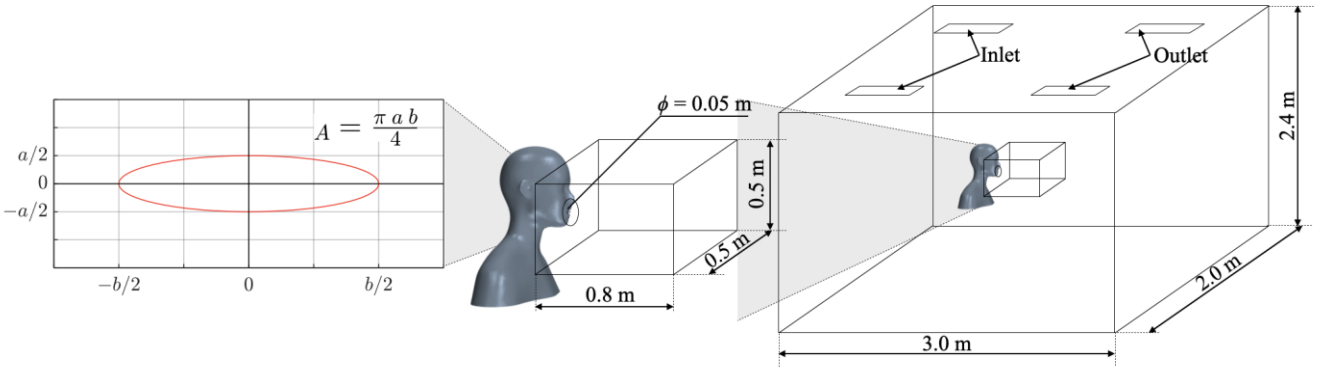

Figure 4 Geometry modeling of coughing human, chamber, and experiment room for numerical simulation.

The detailed numerical methods and boundary conditions are summarized in Table 2. The three-dimensional Reynolds-averaged Navier-Stokes equations for the conservation of mass, momentum, and energy are solved using the realizable k–ε model A second-order upwind scheme was used as the convection term in the discretization scheme. The pressure–velocity coupling for the continuous fluid was solved using the SIMPLE algorithm (Leonard 1979).

The room temperature and temperature of the airflow generated by coughing were assumed to be 24 and 32 ℃ (75.2 and 89.6 °F), recpectively. The time-series data of the airflow center corresponding to Point 1 (P_1) of x/b = 2.5, of the result obtained from the ensemble average distribution was used as the boundary condition of the mouth opening. In addition, a correction factor c was introduced as shown in Equation 4.

$$v_{\mathrm{CFD}}(t) = c \cdot \langle v_{\mathrm{EXP},P_1}(t) \rangle \quad (4)$$

where, $v_{\mathrm{CFD}}(t)$ is the time-series velocity data for the boundary condition in CFD analysis, and $v_{\mathrm{EXP,P1}}(t)$ is the time-series velocity result at Point1 obtained by ensemble average. After the stable-state calculation of the indoor continuous fluid under ventilation converged, the transient calculation was performed for 2 s at Δt = 0.001 s intervals.

Table 2. Numerical methods and boundary conditions

Program	STAR-CCM+ 14.06
Turbulence model	Realizable k–ε turbulence model
Mesh model	Trimmed mesh, prism layer
Difference scheme	Convection term: second-order upwind
Algorithm	SIMPLE
Buoyancy model	Boussinesq approximation
Time	Indoor airflow: steady-state Coughing: transient (Δt = 0.001 s)
Inlet	Structure: 0.5 × 0.05 m^2 (1.64 × 0.16 ft^2), Velocity inlet: 0.05 m/s (0.16 ft/s), Turbulence intensity: 5%, Turbulence length: 0.07 × D_{h} m, Temperature: 24 °C (75.2 °F)
Outlet	Pressure outlet: static pressure = 0 Pa
Wall / Human body	Adiabatic
Mouth opening	Velocity inlet: $v_{\mathrm{CFD}}(t)$, ensemble average of time-series velocity $\langle v_{\mathrm{EXP},P_1}(t) \rangle$ with correction factor C Turbulence intensity: 10%, Turbulence length: 0.07 × D_{h} m, Temperature: 32 °C (89.6 °F)

RESULTS

Time-series ensemble average of velocity

The right side of Figure 3 shows an example of the ensemble average result of the velocity distribution obtained from the PIV experiment. If the direction of airflow was not clearly identified, it was excluded from the calculation of the ensemble average. It was confirmed that the maximum wind speed was formed approximately at the position of x/b = 2.5. In PIV techniques, velocity is calculated based on the movement of oil particles that were captured by image. On the other hand, because the airflow generated by coughing does not contain oil particles, it is difficult to clearly measure the wind speed at the interface of the mouth.

Because there was a difference in the maximum velocity of ensemble average between males and females, the analysis was performed by separating gender. Figure 5 shows the time-series ensemble velocity at Point 1 (P_1) to Point 4 (P_4). The color region is the standard deviation range of the ensemble average. The maximum wind speed was formed approximately at the position of P_1 (x/b = 2.5, z/b = 0), showing 10.7 m/s (35.1 ft/s) for male and 8.4 m/s (27.6 ft/s) for female.

Figure 6 shows the ensemble average result of velocity profile (x/b = 2.5) when the maximum speed appeared (t = 0.057 s). As coordinate axes transformation had been performed, the ensemble average of airflow generated by coughing showed symmetric with respect to z/b = 0.

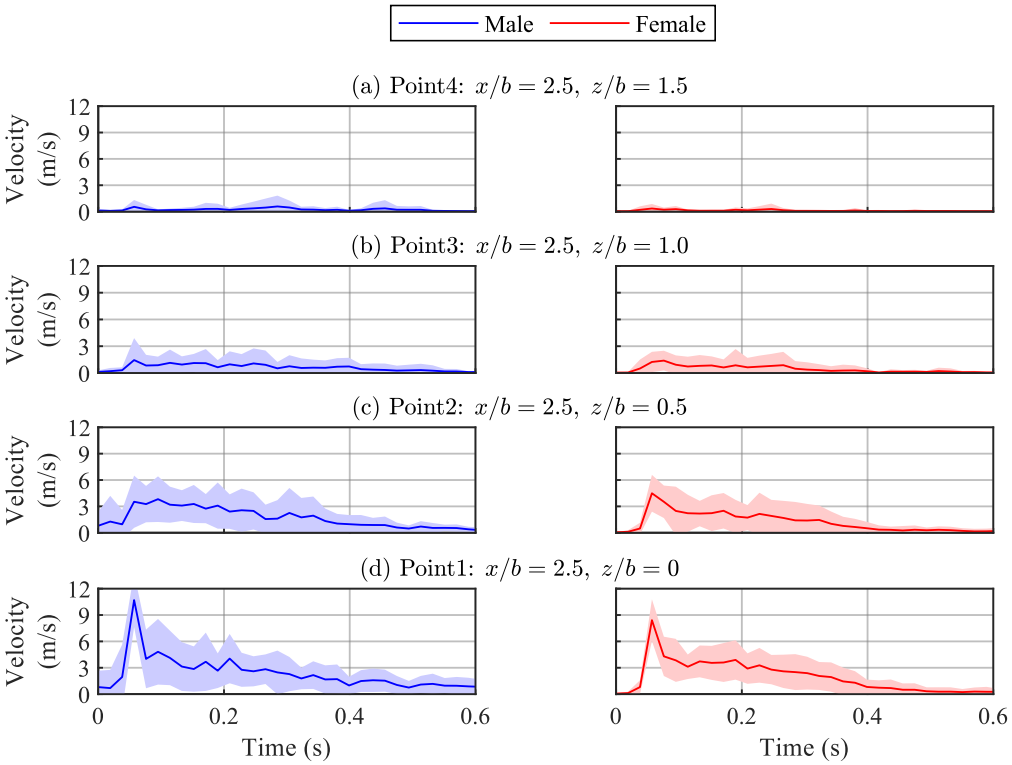

Figure 5 Time-series air velocity at each point.

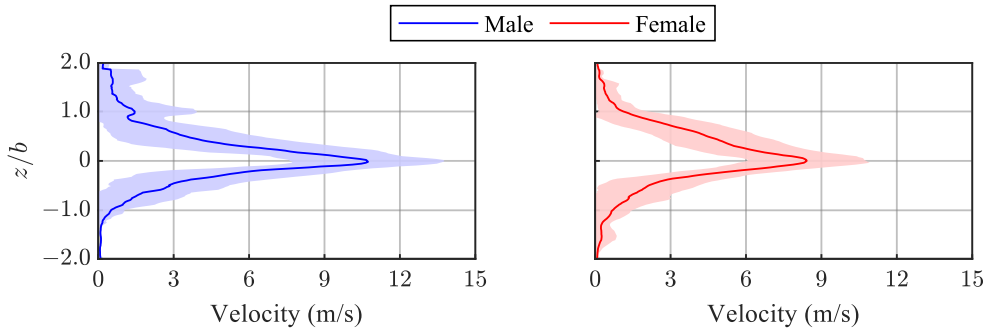

Figure 6 Air velocity distribution at peak velocity (t = 0.057 s).

Application of correction factor in CFD boundary condition

The CFD simulation was performed by setting the time-series velocity data as the boundary condition, taking into account the correction factor and velocity at the position P1 of the ensemble average result. The correction factor was set from 1 to 2. Because the maximum velocity is considered to be the most important factor in the dispersion of droplets and droplet nuclei, the maximum wind speed at the P_1 location was examined and compared. Figure 7 shows the maximum velocity at the P_1 position according to the correction factor. By linear regression, the correction factors where the maximum velocity of P1 equal to the maximum velocity of the ensemble average were estimated to be 1.93 for males and 2.02 for females.

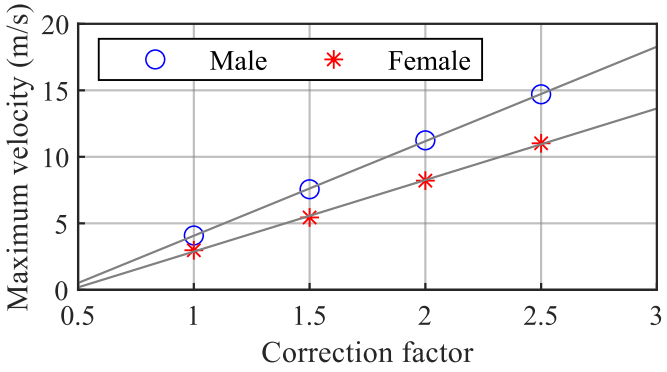

Figure 7 Maximum velocity at Point1 in the result of CFD considering correction factor.

Validation of boundary conditions of coughing

CFD analysis was performed again by applying the correction factor obtained in the previous section and verified by comparing it with the result of ensembled average. Figure 8 shows the comparison of the time-series velocity results at the P_1 position between CFD and ensemble average of experiments.

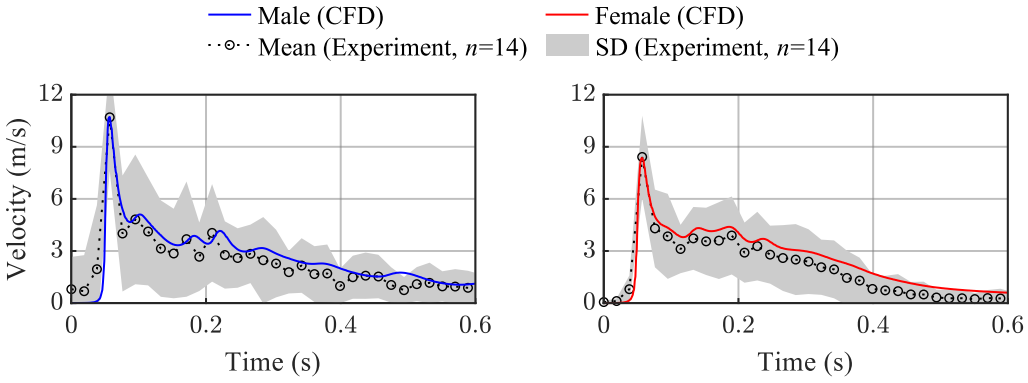

Figure 8 Comparision of time-series velocity results at P_1 between reporudced coughing model by CFD and ensemble average by experiment.

The RMSE calculation of Equation (5) was used to evaluate the degree of reproducibility of CFD. As a result, the RMSE values were 0.42 m/s (1.38 ft/s) for male and 0.38 m/s (1.25 ft/s) for female.

$$\mathrm{RMSE} = \sqrt{\frac{\sum_{i=1}^{m}\sum_{j=1}^{n}\left(\langle v_{\mathrm{EXP},P_i}(t_j)\rangle - v_{\mathrm{CFD},P_i}(t_j)\right)^2}{m\,n}} \tag{5}$$

where, n is the total number of time interval data of the emsemble average, and m is the number of positions P_1 to P_4. The data interval of the ensemble average result was 0.019 s.

DISCUSSION

Fig. 1 shows the maximum velocity according to the distance x from the mouth of person (0, 0). v_{CFD,P_1} and $< v_{\mathrm{EXP},P_1} >$

represents the result of CFD considering the correction factor and without considering the correction factor, respectively. The dotted line and gray area indicate the mean and standard deviation of the ensemble average of experimental data. The maximum velocities of the boundary condition considering the correction factor were 20.65 m/s (67.75 ft/s) for men and 16.97 m/s (55.68 ft/s) for women, but the formed maximum wind speeds were 15.2 m/s (49.9 ft/s) and 12.8 m/s (42.0 ft/s) in front of the mouth, respectively.

If the time-series velocity results obtained from the PIV experiment are directly used as the boundary condition in CFD analysis, the dispersion and reaching distance of droplet and droplet nuclei would be underestimated. In addition, it is necessary to model the structure of the human nasal cavity and mouth to reproduce the Vena contracta phenomenon (Vansciver, Miller, and Hertzberg 2011; Mahjoub Mohammed Merghani et al. 2021). Moreover, depending on the presence or absence of the detailed modeling, it is necessary to examine whether the dispersion characteristics of the droplets and droplet nuclei show a significant difference.

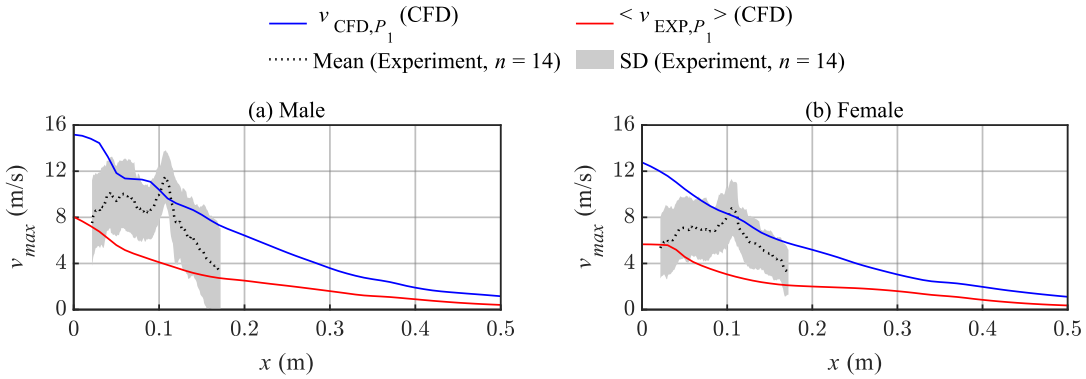

Figure 9 Maximum velocity according to distance from the mouth.

CONCLUSION

The characteristics of airflow generated by coughing, the results obtained from PIV, were analyzed and the ensemble average was derived. Using the derived ensemble average velocity result and correction factor, the airflow characteristics were reproduced by setting the boundary condition in CFD analysis. The time-series velocity distribution by CFD simulation was reproduced with 0.38–0.42 m/s (1.25–1.38 ft/s) RMSE compared to the ensemble average obtained in the experiment. As a future task, the particle size distribution of droplets generated by coughing is measured, and the results are applied in CFD analysis tu understand the characteristics of droplet and droplet nuclei dispersion.

REFERENCES

Gralton, Jan, Euan Tovey, Mary Louise McLaws, and William D. Rawlinson. 2011. "The Role of Particle Size in Aerosolised Pathogen Transmission: A Review." *Journal of Infection* 62 (1): 1–13.

Gupta, J. K., C. H. Lin, and Q. Chen. 2009. "Flow Dynamics and Characterization of a Cough." *Indoor Air* 19 (6): 517–25. Han, Mengtao, Ryozo Ooka, Hideki Kikumoto, Wonseok Oh, Yunchen Bu, and Shuyuan Hu. 2021. "Measurements of Exhaled Airflow Velocirty via Human Coughs Using Particle Image Velocimetry (PIV) (Submitted)."

He, Qibin, Jianlei Niu, Naiping Gao, Tong Zhu, and Jiazheng Wu. 2011. "CFD Study of Exhaled Droplet Transmission between Occupants under Different Ventilation Strategies in a Typical Office Room." *Building and Environment* 46 (2): 397–408.

Leonard, B.P. 1979. "A Stable and Accurate Convective Modelling Procedure Based on Quadratic Upstream Interpolation." *Computer Methods in Applied Mechanics and Engineering* 19 (1): 59–98.

Mahjoub Mohammed Merghani, Khansa, Benoit Sagot, Evelyne Gehin, Guillaume Da, and Charles Motzkus. 2021. "A Review on the Applied Techniques of Exhaled Airflow and Droplets Characterization." *Indoor Air* 31 (1): 7–25.

Qian, H., and Y. Li. 2010. "Removal of Exhaled Particles by Ventilation and Deposition in a Multibed Airborne Infection Isolation Room." *Indoor Air* 20 (4): 284–97.

Richmond-Bryant, Jennifer. 2009. "Transport of Exhaled Particulate Matter in Airborne Infection Isolation Rooms." *Building and Environment* 44 (1): 44–55.

Scharfman, B. E., A. H. Techet, J. W.M. Bush, and L. Bourouiba. 2016. "Visualization of Sneeze Ejecta: Steps of Fluid Fragmentation Leading to Respiratory Droplets." *Experiments in Fluids* 57 (2): 1–9.

Vansciver, Meg, Shelly Miller, and Jean Hertzberg. 2011. "Particle Image Velocimetry of Human Cough." *Aerosol Science and Technology* 45 (3): 415–22.

Xu, Chunwen, P. V. Nielsen, Li Liu, Rasmus L. Jensen, and Guangcai Gong. 2017. "Human Exhalation Characterization with the Aid of Schlieren Imaging Technique." *Building and Environment* 112 (February): 190–99.

Yu, Ignatius T.S., Yuguo Li, Tze Wai Wong, Wilson Tam, Andy T. Chan, Joseph H.W. Lee, Dennis Y.C. Leung, and Tommy Ho. 2004. "Evidence of Airborne Transmission of the Severe Acute Respiratory Syndrome Virus." *New England Journal of Medicine* 350 (17): 1731–39.

Zhu, Shengwei, Shinsuke Kato, and Jeong Hoon Yang. 2006. "Study on Transport Characteristics of Saliva Droplets Produced by Coughing in a Calm Indoor Environment." *Building and Environment* 41 (12): 1691–1702.